Journal of
Molluscan Studies

The Malacological Society of London

Journal of Molluscan Studies (2015) **81**: 356–364. doi:10.1093/mollus/eyv001
Advance Access publication date: 16 February 2015

Embryonic and larval development of the New Zealand bivalve *Paphies ventricosa* Gray, 1843 (Veneroida: Mesodesmatidae) at a range of temperatures

Kendall Gadomski[1], Henrik Moller[2], Michael Beentjes[3] and Miles Lamare[1]

[1]*Department of Marine Science, University of Otago, Dunedin, New Zealand;*
[2]*Centre for Sustainability (CSAFE), University of Otago, Dunedin, New Zealand; and*
[3]*National Institute of Water and Atmospheric Research, 38 Harrow Street, Dunedin, New Zeland*

Correspondence: M. Lamare; e-mail: miles.lamare@otago.ac.nz

(Received 3 June 2014; accepted 14 December 2014)

ABSTRACT

Paphies ventricosa is a large (up to 150 mm shell length) surf clam endemic to New Zealand, with a geographically patchy distribution. Using scanning electron microscopy and light microscopy, its fertilization, embryonic and larval development were observed at three culturing temperatures (12, 16 and 20 °C). The progress of development follows that previously described for the family Mesodesmatidae, with *P. ventricosa* having a small egg (63–70 μm), with a 83–102 μm trochophore stage observed at 15 h, and a 100 μm D-veliger larva observed at 22 h at 12 and 16°C, and 37 h at 20 °C. At 20 °C, the pediveliger larval stage was reached by 31 d. While the morphology of the embryonic and larval stages of *P. ventricosa* is typical for bivalves, we show that in this species the shell field invagination occurs in the gastrula stage and that the expansion of the dorsal shell field occurs during gastrulation, with the early trochophore having a well-developed shell field that has a clearly defined axial line between the two shell lobes. The growth of *P. ventricosa* larvae cultured at 12, 16 or 20 °C over 39, 33 and 31 d respectively, was faster at warmer temperatures. Using the temperature quotient Q_{10} at day 27 to quantify the response to temperature, values of $Q_{10} = 1.82$ for the range 12–16 °C and $Q_{10} = 2.33$ for the range 16–20 °C were calculated. Larval shape was not temperature dependent, suggesting that the smaller larvae found at colder temperatures reflect a slowing of larval development, rather than physiological damage by temperature resulting in abnormal larval development.

INTRODUCTION

Paphies ventricosa Gray, 1843 (Veneroida: Mesodesmatidae), known by the Māori name toheroa, is a large surf clam (up to 150 mm in shell length (SL)) endemic to New Zealand. The species has a broad latitudinal distribution ranging between 34° 31′ S and 46° 20′ S, although only three significant populations presently exist, these being physically separated by up to 700 km. The species is restricted to high-energy dissipating beaches that are on western-facing fully-exposed coasts made of fine sand (0.25 mm average grain size) (Rapson, 1952; Cassie, 1955). *Paphies ventricosa* population sizes throughout New Zealand have decreased substantially over the past century. For example, Greenway (1972) estimated that the northern population had declined from an estimated 10,000,000 individuals in 1964 to an estimated 1,000,000 in 1971. The reasons for the decline are poorly understood, but substantial over-fishing in the first half of the 20th century (Rapson, 1952), habitat degradation and disturbance from beach traffic are contributors (Beentjes, Carbines & Willsman, 2006).

Recruitment has also been identified as an important problem for the future of the species (Beentjes *et al.*, 2006), given the small, reducing population sizes and the geographically fragmented distribution of the three main populations, which potentially cause variable larval supply A key aspect in understanding recruitment in *P. ventricosa* is quantifying processes controlling larval supply, which include larval production, transport and factors influencing the number of larva completing development to settlement. For bivalves, a key factor in the last of these is the rate of larval development which, in turn, is primarily influenced by temperature and food concentration (Pechenik, 1990; Pechenik *et al.*, 1990; Widdows, 1991).

This study aims to increase our understanding of embryonic and larval development in *P. ventricosa*, and the role of temperature in the rate of development. While there are brief descriptions of various preveliger developmental stages (Rapson, 1952; Redfearn, 1974, 1982), a detailed description of early embryonic and larval development and morphology of *P. ventricosa* is lacking. Redfearn (1982) used scanning electron microscopy (SEM) to describe larval shell development in the veliger, noting that *P. ventricosa* reaches the straight-hinged veliger stage after 24–48 h, and completes development to metamorphosis in 22 d at 25 °C. Importantly, the development processes described for *P. ventricosa* by Redfearn (1982) were at temperatures associated with the northern limit of the species (i.e. 18–25 °C), with no

description available for larvae at temperatures associated with the species' southern range (i.e. 12–16 °C). The effects of temperature on bivalve larval development have been established in a number of species, with rates typically increasing with temperature (Cataldo *et al*., 2005; Cragg, 2006; Sánchez-Lazo & Martínez-Pita, 2012); it is therefore likely that development processes are slower in the colder southern regions.

Embryonic and larval development in bivalves have been well described (Sastry, 1979; Kasyanov *et al*., 1998), with light microscopic techniques contributing to a clear understanding of patterns of fertilization, spiral cleavage (Lambert, 2010) and the functional morphology of the blastula, gastrula and veliger stages (e.g. in *Ostrea edulis*, Waller, 1981). This technique has also allowed the timing of these key developmental milestones to be determined for ecologically and economically important species (review by Ackerman *et al*., 1994). The use of SEM and transmission electron microscopy techniques to examine early developmental processes in bivalves is less common, but has been used to view spermatozoa (Mouëza & Frenkiel, 1995; Mouëza, Gros & Frenkiel, 1999), embryonic and larval morphology (Zardus & Morse, 1998; da Costa, Darriba & Martínez-Patiño, 2008), ciliation patterns (Eyster & Morse, 1984; Chaparro, Thompson & Emerson, 1999; Mouëza *et al*., 1999; Mouëza, Gros, Frenkiel, 2006), larval shell differentiation (Eyster & Morse, 1984; Mouëza *et al*., 2006; Aranda-Burgos *et al*., 2014), internal anatomy (Zardus & Morse, 1998) and larval shell development and hinge morphology (Redfearn, 1982; da Costa *et al*., 2008; Arellano & Young, 2009).

Here, a detailed description of the development of *P. ventricosa* is made using both light microscopy and SEM techniques. To gain an understanding of the role of temperature in embryonic and larval development across the natural thermal range (i.e. 12–25 °C), we examine the effects of three environmentally relevant temperatures (12, 16 and 20 °C) on larval growth. This is done by quantifying, at each of the three temperatures: (1) timing of key development processes using developmental schedules; (2) larval size over the free-swimming period and (3) differences in larval shell morphology (to understand if temperature not only changes the pace of development but also key developmental processes such as shell formation). We compare our measurements with those previously made for *P. ventricosa* larvae at 25 °C by Redfearn (1982) and discuss the role of temperature on larval development and its implications for larval supply in the species across its geographic range.

MATERIAL AND METHODS

Animal collection and conditioning

In October 2012, 20 adult *Paphies ventricosa* (100–110 mm SL) were collected from Oreti Beach (46.479°S, 168.252°E), Southland, New Zealand. Animals were extracted by hand during low tide and transported to the Portobello Marine Laboratory, Dunedin, in seawater-filled buckets. In the laboratory, individuals were placed at densities of 10 individuals per tank into 4 circular flow-through 116-l tanks (43.5 × 58.5 cm, flow 3 l min^{-1}) filled to 35 cm depth with Oreti Beach sand. Oxygen concentrations were maintained through continuous aeration. Animals were conditioned for spawning by feeding daily with a mixed algal culture (*Tetraselmis chui*, *Isochrysis galbana*, *Pavlova lutheri*, *Chaetoceros muelleri* and *Skeletonema marinoi*). At feeding, water flows were turned off, tanks were cleaned by siphoning off 5 l of water, and 5 l of mixed algae were then added to each tank to give a final concentration of 8–10 × 10^5 algal cell ml^{-1} in each tank. The relative proportions of each algal species depended on the availability of cultures. During feeding, the tanks were aerated by bubbling, in order to maintain mixing and water quality. Water flows were restored once the animals had cleared the water, or after 4 h, whichever came first. Animals were conditioned for *c*. 7 weeks.

Spawning

For spawning, animals were removed from their tanks and placed into 15 cm deep flow-through trays filled with 25 l of flowing seawater and fitted with air stones for additional aeration. Spawning was induced by an intramuscular crystalline serotonin (5-hydroxytryptamine [5-HT]) injection, similar to methods described by Gibbons & Castagna (1984) and Hirai *et al*. (1988). After turning off seawater flow, animals were given an initial 0.4 ml injection of a 2 mM solution of 5-HT (Sigma-Aldrich®) in 1 μm filtered seawater (FSW) into the anterior adductor muscle (AAM) and placed back into the aerated spawning trays. Injected animals were observed for the start of spawning and then given an additional 0.2 ml injection of 2 mM 5-HT into the AAM every 30 min, for up to 90 min postinitial injection (up to a total of 1 ml injection volume) or until a good spawning was observed. Spawning was allowed to occur within the spawning trays and settled eggs were collected. Sperm were collected from spawning males immediately prior to sperm counting and fertilization.

Larval rearing

Eggs were pooled from five females and sperm collected from three males. For fertilization, the pooled eggs were mixed in 1 l of 0.22 μm FSW and sperm added to obtain a final concentration of 10^6 sperm ml^{-1}. Fertilization was confirmed by the breakdown of the germinal vesicle and the appearance of the fertilization envelope and polar body. Following fertilization, the top 70% of the beaker volume was poured off into a 5-l beaker, leaving behind any residual debris. Fertilized eggs were further diluted with 0.22 μm FSW to a density of 15 eggs ml^{-1} and split into nine 500-ml lidded jars, each filled to a volume of 450 ml.

The cultures were then reared simultaneously in the same temperature-controlled room at one of three temperature treatments, 12 °C (temperature-controlled water bath), 16 °C (controlled-temperature room ambient temperature) and 20 °C (temperature-controlled water bath). Each treatment was replicated three times. Water changes and feeding were carried out every third day. Larvae were filtered and rinsed using a larval filter stack fitted with a 50-μm mesh filter. Cleaned larvae were rinsed off the filter into a jar half filled with fresh FSW and topped up to a volume of 450 ml. Following the water change, larvae were fed cultured *T. chui* at a concentration of 10,000 cells ml^{-1}. The algal concentration was calculated immediately before each feeding using a haemocytometer.

Larval photography and larval morphometrics

Early development was observed frequently over the first 48 h postfertilization in 1 ml subsamples of the culture, then every third day. Developmental stages were photographed alive using an Olympus BX51 compound microscope fitted with an Olympus Colorview III™ camera and AnalySIS LS Research software (Olympus Corporation). Larval shell morphometric measurements of total SL, total shell height (SH) and shell hinge-line length (HL) were taken (Fig. 1I) as described by Redfearn (1982), using the software ImageJ 1.38x (NIH, USA). For statistical comparison with measurements made by Redfearn (1982), data contained in the published figures were digitized using the software Digitizelt (Braunschweig, Germany).

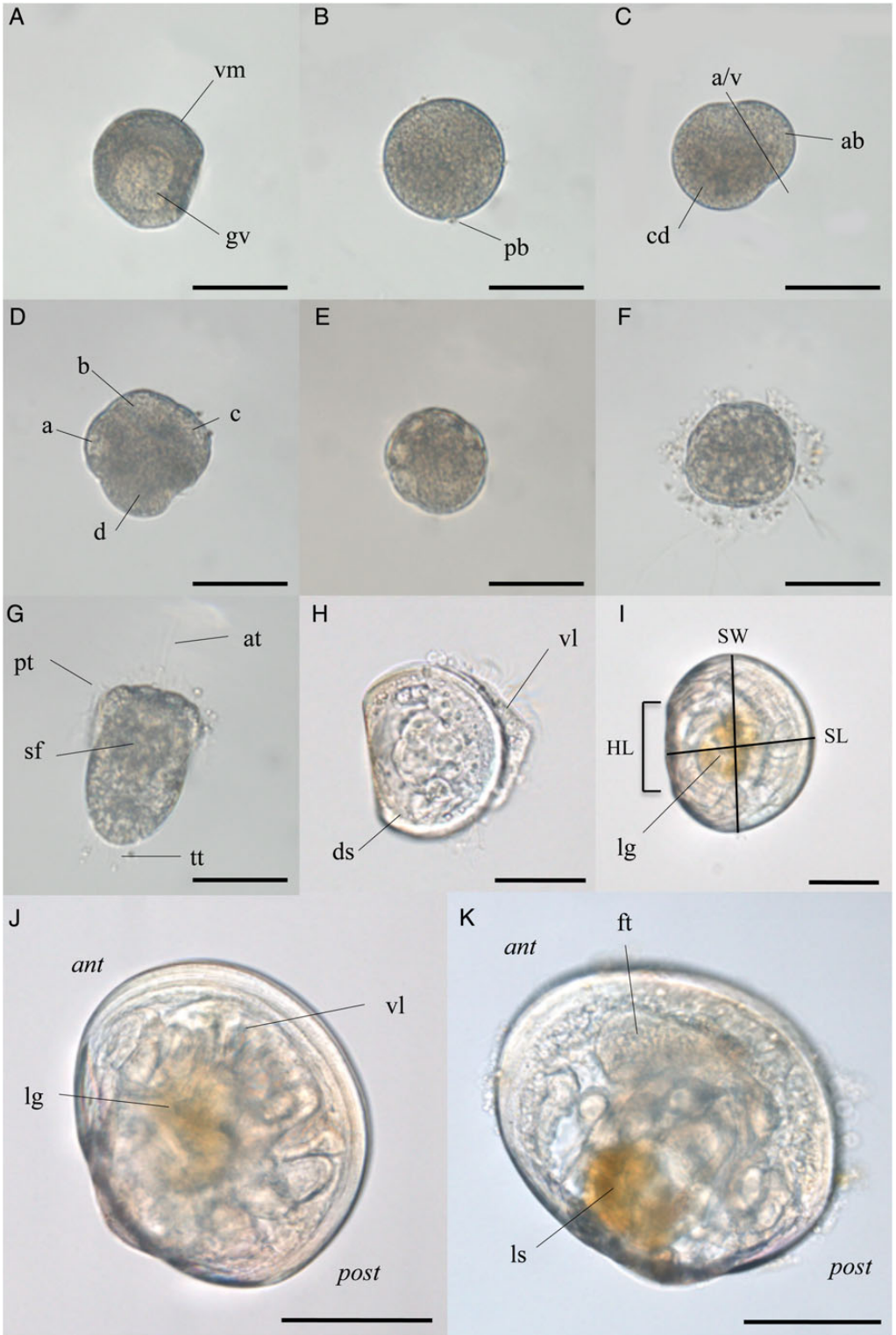

Figure 1. Light micrographs of egg and embryonic and larval developmental stages of *Paphies ventricosa*. All were reared at 16 °C except for **J** and **K**, which were reared at 20 °C. **A.** Unfertilized egg, with vitelline membrane (vm) and germinal vesicle (gv). **B.** Fertilized egg at 15 min with polar body (pb). **C.** Two-cell embryo at 30 min with larger CD blastomere (cd) and smaller AB blastomere (ab) dividing along animal-vegetal axis (*a*/*v*). **D.** Four-cell embryo at 60 min with blastomeres *a* to *d* labelled. **E.** Eight-cell embryo at 4 h viewed from vegetal pole. **F.** Hatched blastula at 6 h. **G.** Trochophore stage at 16 h, with well-developed prototroch (pt), telotroch (tt) and apical tuft (at). Region of ventral shell field (sf) is indicated. **H.** Straight-hinged D-larva at 3 d with prodissoconch I (ds) and extended velum (vl). **I.** Straight-hinged D-larva at 15 d with larval gut (lg). Larval shell with shell length (SL), shell height (SW) and hinge line (HL) dimensions indicated. **J.** Twenty-day umbo larva with larval gut (lg), retracted velum (vl). Posterior (post) and anterior (ant) ends are indicated. **K.** Thirty-day old pediveliger larva with foot retracted (f). Scale bars **A–I** = 50 μm; **J, K** = 100 μm.

Scanning electron microscopy

Samples were fixed in 10% neutral buffered formalin in seawater and processed in a Bal-Tec CPD-030 critical-point drier (Bal-Tec AG), mounted on stubs and sputter coated using an Emitech K575X Peltier-cooled high-resolution sputter coater (EM Technologies). Mounted samples were photographed using a JEOL 6700F FE-SEM field-emission SEM, with the lower secondary detector set to high magnification mode. Images were postprocessed using Gimp v. 2.8 software (GNOME foundation, USA) to improve contrast and to black out the background.

Statistical analyses

Significant differences in larval shell measurements (SL, SW and HL) over time and among temperature treatments were tested in a univariate repeated-measures analysis of variance (ANOVA), using data on the days when measurements were available for all replicates (days 6, 9, 15, 18, 21, 24 and 27). Tests for sphericity (homogeneity of variances among groups) were made using Mauchly's sphericity test (W) (Mauchly, 1940) and departures from the assumption of sphericity were corrected using the Greenhouse-Geisser correction (ϵ). A significant interaction between temperature and day necessitated a statistical examination of the effect of temperature treatment on separate days by one-way ANOVA of the transformed data. The effect of temperature on the relationship between total larval length and larval height was examined using an analysis of covariance (ANCOVA) on $\ln(x)$-transformed measurements. All statistical analyses were undertaken using the software JMP v. 10.0 (SAS Institute, USA).

RESULTS

Embryonic and larval development

Spawned eggs had an average diameter of 67.1 μm (range 60.1–75.1 μm) and before fertilization were often pear-shaped. A thin vitelline layer of 2.0–2.5 μm was present, with no jelly coat visible (Fig. 1A). The germinal vesicle was prominent, measuring 40 μm in diameter. Following fertilization, a polar body formed within 10–15 min, with the first cleavage occurring within 1 h of fertilization (Figs 1C, 2A). The cleavage plane along the animal-vegetal axis was uneven and resulted in the characteristic two-cell embryo with the larger CD blastomere and the smaller AB blastomere, with the polar body located at the animal end of the cleavage plane (Figs 1C, 2A). Subsequent cell divisions followed spiral cleavage as described for other bivalve embryos, with the second cleavage plane perpendicular to the first, resulting in four blastomeres (Fig. 1D) and the third cleavage to the eight-cell stage resulting in four smaller daughter blastomeres visible when viewed from the vegetal pole (Fig. 1E). Dexiotropic and laetropic spiral divisions gave rise to a 75 μm ciliated blastula (Figs 1F, 2B) by 15 h at 20 °C. The ciliated blastula retained the polar lobe and had a sparse, uneven cover of cilia (length 18–20 μm) running almost equatorially around the embryo body, marking the initial development of the prototroch (Fig. 2B). The formation of a blastopore measuring 10.5 μm across was observed in slightly larger blastulae (80–85 μm length), located ventral-posteriorly to the developing prototroch (Fig. 2C). At the same time, the shell field invagination had formed dorso-posteriorly, measuring 30 μm length with a depth of 7–8 μm. Early trochophores (Fig. 2E) measuring 83 μm in length have a well-developed shell field 45 μm wide, containing a two-lobed shell pellicle of wrinkled periostracum, each lobe separated along the axial line. Cilia surrounded the shell field, with the cilia of both prototroch and telotroch developed. During the expansion of the shell field, the blastopore was displaced ventro-posteriorly. Early trochophore larvae (Fig. 2D) measuring 85 μm in length had a well-developed prototroch measuring 95–100 μm (cilia length 23 μm), postoral cilia (cilia length 16 μm) and a telotroch (cilia length 21 μm). At the same time, the developing shell field was apparent, lying dorsal to the blastopore (Fig. 2E). Trochophore larvae observed in samples at 15-h postfertilization were 102 μm in length (Figs 1G, 2F). At this stage, larvae had a well-developed prototroch with cilia 26 μm in length (Fig. 2F). The prototroch divided the larval body into the anterior pretrochal region and the posterior posttrochal region. The apical plate of the pretrochal region contained the apical sense organ (not clearly visible in this preparation), which gave rise to sensory apical cilia extending to 67 μm (Fig. 1G). At this stage the posttrochal region was almost covered by the dorsally-expanding shell rudiment, which tended to flatten the larval body laterally. During this expansion the mouth was retained in a ventral position. Early veliger larvae at 22 h had a fully developed velum 110–120 μm in length (Fig. 2G). Well-developed postoral cilia (21 μm long) and postanal tuft cilia (24 μm long) were present. The rudimentary shell had the characteristic D-larval form with a straight, dorsal hinge line 65 μm in length (Figs 1H, 2H). The morphology of the larval-shell hinge (Fig. 1I, J) was as described by Redfearn (1982), with the straight-hinged D-larva having a hinge consisting of up to 25–30 regularly spaced teeth (Fig. 2I), while at the umbo stage the hinge consisted of 13 evenly spaced teeth (2.2 × 3.5 μm) along a hinge line of 67 μm (Fig. 2I, insert).

Temperature and larval development

Progression through the early embryonic stages was temperature dependent (Table 1), with blastulae observed at 15 h postfertilization at 20 °C, while by the same time embryos had reached the trochophore stage at 12 and 16 °C. D-hinge veliger larvae were first observed at 22 h postfertilization in the 12 and 16 °C treatments, and at 37 h at 20 °C. Later larvae developed more quickly in the warmer treatments, with umbo larvae observed at 21, 15 and 12 d postfertilization at 12, 16 and 20 °C, respectively. Larvae reached the pediveliger stage (recognized by a protruding larval foot) after 31 d at 20 °C, but pediveligers were not observed by 39 d in the two colder treatments.

Total larval SL increased from 65 μm at 2 d postfertilization to a maximum of 269 μm after 30 d (Fig. 3A). Differences in larval size among temperature treatments were most apparent at day 15 when the larvae were 100 μm in length, a size at which larvae at 20 °C progressed from straight-hinge D-larvae to umbo larvae. The maximum size of larvae reared at 20 °C (269 μm) was about 1.5 times larger than those reared at 12 °C (170 μm) and 16 °C (196 μm). A repeated-measures ANOVA of change in larval size undertaken on those days when measurements were available for all replicates (days 6, 9, 18, 21, 24 and 27) showed that, for total SL, there was a significant effect of temperature ($P < 0.001$), although the effect of temperature was dependent on day (Temperature × Day, $P < 0.001$; Supplementary material, Table S1A). A significant ($P < 0.05$) difference in size among temperatures was first apparent on day 18 and, by day 27, larvae reared at 20 °C were significantly larger. A similar pattern of changes in SH was observed among temperature treatments (Fig. 3B), with those larvae reared at 20 °C significantly larger than those at 12 and 16 °C. Larval height increased significantly over time ($P < 0.001$; Supplementary material, Table S1B), with the height significantly different among temperature treatments. The effect of temperature varied with time (Temperature × Day, $P < 0.001$) and reflected the divergence of height after day 9. Larval HL (Fig. 3C) was significantly longer in larvae reared at 20 °C compared with those reared at the colder temperatures ($P = 0.001$; Supplementary material,

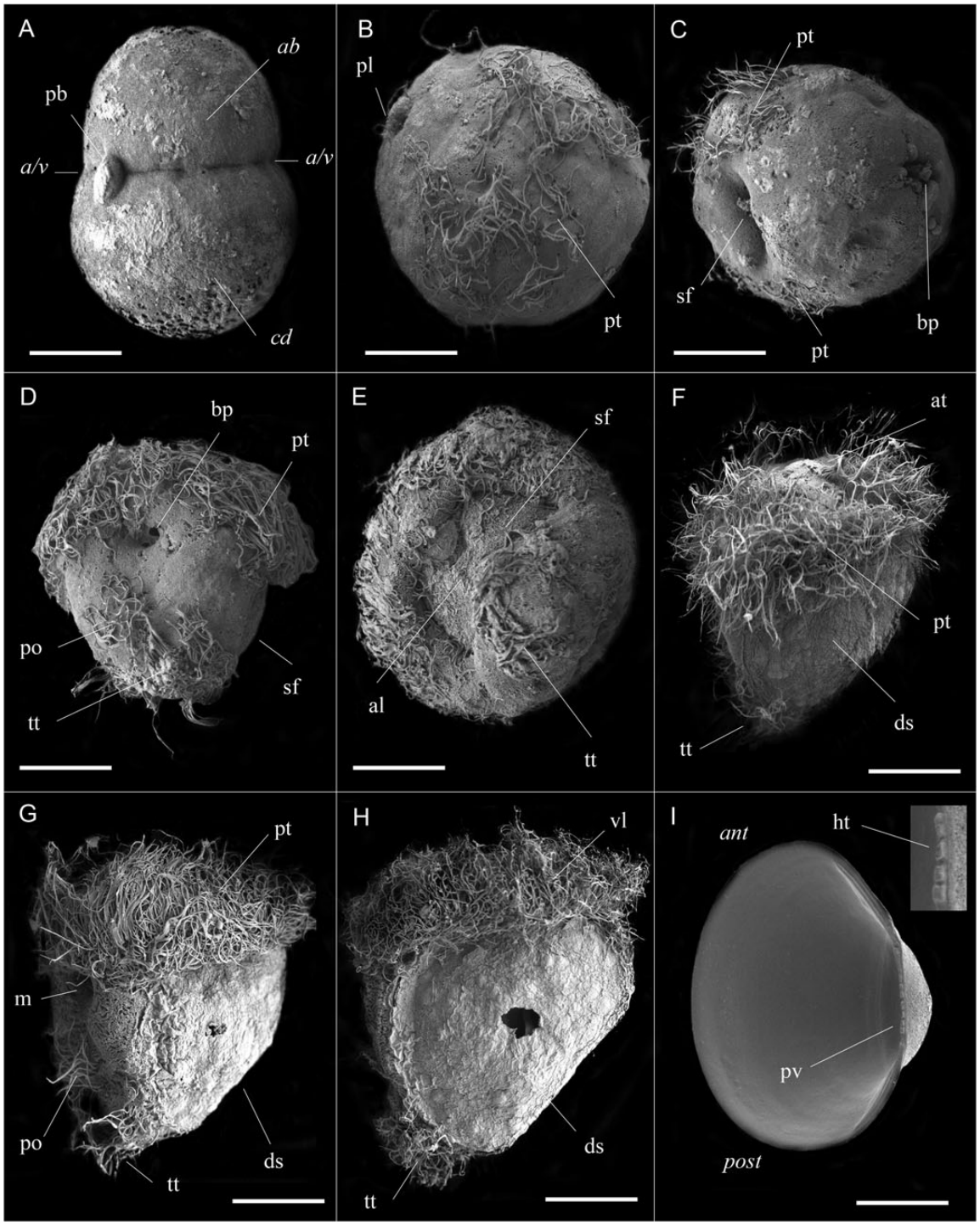

Figure 2. Scanning electron micrographs of embryonic and larval developmental stages of *Paphies ventricosa*. All were reared at 16 °C except for **H** and **I**, which were reared at 20 °C. **A.** Two-cell embryo at 1 h, with larger *cd* blastomere and smaller *ab* blastomere. Polar body (pb) is located on cleavage plane (animal-vegetal axis, *a/v*) at animal pole. **B.** Blastula at 5 h with cilia of developing prototroch (pt) starting to cover equatorial region of embryo. Polar lobe (pl) still visible at vegetal pole. **C.** Late gastrula at 8 h with blastopore (bp) located dorso-posterially to developing prototroch (pt), with shell field invagination (sf) ventro-posterior. **D.** Early trochophore at 15 h; ventral view with well-developed prototroch (pt), teletroch (tt) and postoral (po) cilia. Shell field (sf) just visible on dorsal surface. **E.** Early trochophore at 15 h, dorsal view with shell field (sf) consisting of two-lobed shell pellicle of noncalcified wrinkled periostracum, separated along axial line (al). **F.** Lateral view of late trochophore with well-developed prototroch (pt) and telotroch (tt). Apical tuft (at) discernible. The expanding prodissoconch (ds) has laterally flattened the posttrochal region of larva. **G.** Late trochophore at 22 h. **H.** Early straight-hinged D-larva viewed ventro-laterally. **G** and **H** show well-developed velum (vl), mouth (m), postoral cilia and telotroch (tt). **I.** Late umbo larval shell at 3d with provinculum (pv) and hinge with peg-like teeth (ht) (insert). Posterior (post) and anterior (ant) ends indicated. Scale bars: **A, B, E** = 25 μm; **C, D, F–H** = 30 μm; **I** = 50 μm.

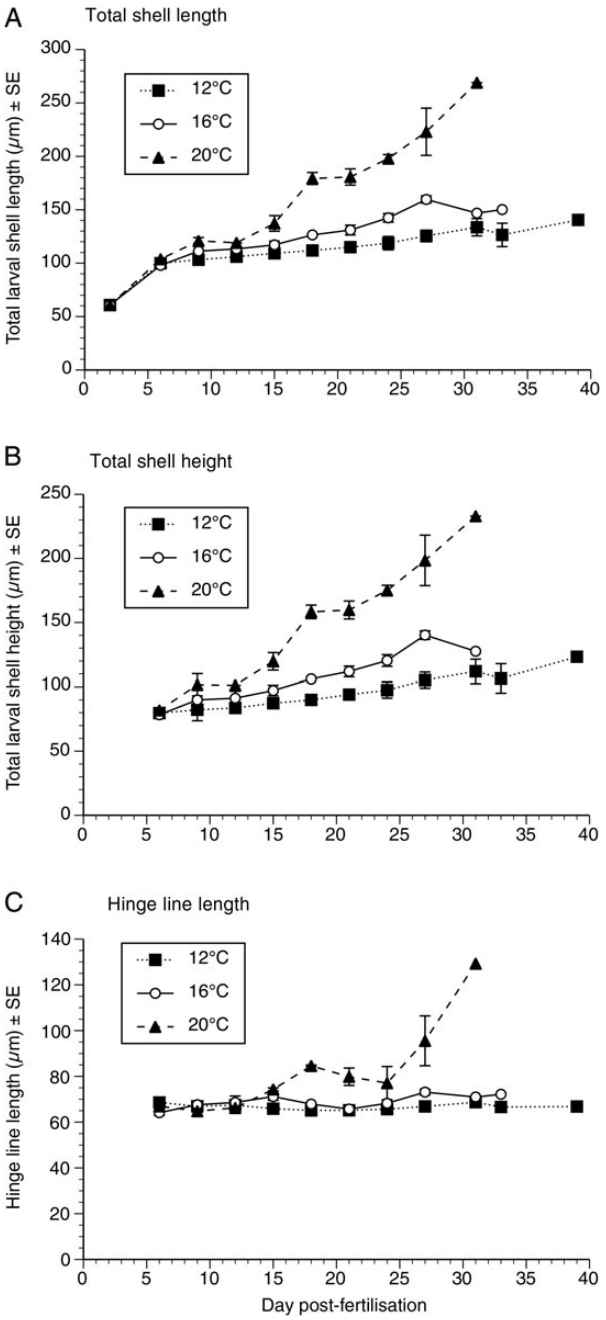

Figure 3. Increase in average shell length (**A**), shell height (**B**) and hinge-line length (**C**) for *Paphies ventricosa* larvae reared over a 39-d period at three temperatures (12, 16 and 20 °C). n = average of three replicate jars, with variable number of larvae measured from each replicate at given time point.

Table S1C), but there was no significant difference between larvae at 12 and 16 °C.

Temperature and posttrochophore larval shell morphometrics

The allometric relationships between larval SL and larval SH for larvae from the three temperature treatments were generally similar (Fig. 4), although ANCOVA indicated that the slopes of the three groups were significantly different (Temperature × SL, $F_{(2,\ 789)} = 8.712$, $P = 0.0002$; Supplementary material, Table S2). A closer inspection of the data suggests that this

Table 1. Time to reach developmental stages for *Paphies ventricosa* larvae reared in the laboratory under three experimental treatments.

Stage	Time to stage		
	12 °C	16 °C	20 °C
Polar-body formation	Not examined	15 min	Not examined
Two-cell	1 h	1 h	1 h
Four-cell	2 h	1 h	1 h
Blastula	*	*	15 h
Trochophore	15 h	15 h	*
D-hinge larvae	22 h	22 h	37 h
Umbonate	21 d	15 d	12 d
Pediveliger	Not reached by 39 d	Not reached by 33 d	31 d

Schedule is based on the time when various larval stages were first observed during regular sampling.

*Not observed in sample.

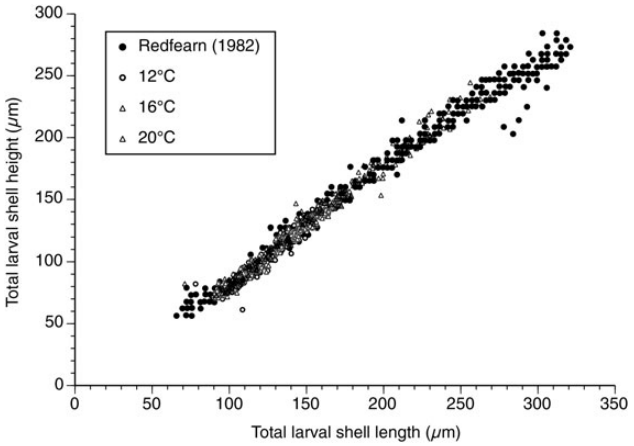

Figure 4. Relationship between shell length and shell height for *Paphies ventricosa* larvae reared over a 39-d period at three experimental temperatures (12, 16 and 20 °C) and at 25 °C (Redfearn, 1982). Allometric relationships ($y = Ax^B$) are: 12 °C, $y = 0.35x^{1.23}$; 16 °C, $y = 0.44x^{1.16}$; 20 °C, $y = 0.57x^{1.09}$; Redfearn (1982), $y = 0.92x^{0.99}$.

result reflects the fact that larvae were only slightly wider for a given length as temperatures increased. This is indicated in the allometric equations of the relationship between SL (x) and SH (y), of which the slope coefficient increases with increasing temperature (i.e. 12 °C, $y = 0.35x^{1.23}$; 16 °C, $y = 0.44x^{1.16}$; 20 °C, $y = 0.57x^{1.09}$). When the data are pooled for the three experimental temperatures and compared with the relationship described by Redfearn (1982) for larvae reared at 25 °C (Fig. 4), the slopes are also significantly different (Source × SL, $F_{(3,\ 1108)} = 12.97$, $P < 0.001$; Supplementary material, Table S2). The results again reflect the greater height of larvae reared at 25 °C, as indicated by the allometric relation $y = 0.92x^{0.99}$ for the measurements of Redfearn (1982).

DISCUSSION

Development of Paphies ventricosa

In this study, we have described the development of *Paphis ventricosa* through the early embryonic to early veliger stages. The developmental processes resemble those previously described for

other members of the family Mesodesmatidae, e.g. *P. australis* (Hooker, 1997) and *P. subtriangulata* (Redfearn, 1987). *Paphies ventricosa* has a medium-sized egg diameter (67 μm), suggesting limited yolk stores, and thus falls within the size range typical of other mesodesmid species with planktotrophic larvae (60–73 μm). *Paphies subtriangulata* has relatively small eggs (56–61 μm, Redfearn, 1987), as does *P. australis* (56.3 μm, Hooker, 1997). For *P. australis* the four-cell and trochophore stages measure 58 and 56.81 μm, respectively (Hooker, 1997). For *P. ventricosa*, trochophores are larger (83–102 μm length) and this stage is first observed 15 h postfertilization. Development times to the D-larval stage are similar in all three New Zealand *Paphies* species, which reach the straight-hinged veliger stage 22–37 h after fertilization in *P. ventricosa* (Redfearn, 1982; present study), 24–36 h in *P. australis* (Hooker, 1997) and 24–48 h in *P. subtriangulata* (Redfearn, 1987). There are few published accounts of embryonic and larval development in other genera of Mesodesmatidae, but most, if not all, have planktotrophic larva. Development of the Pacific species *Mesodesma donacium* has been well described; this species has a small egg (50 μm) that develops to a blastula of the same size by day 1, to a 70-μm D-larva by day 4 and to an umbo larva by day 22 (Carstensen *et al.*, 2006). *Mesodesma mactroides* from the Atlantic coast of South America releases a large number of eggs (5.3 million eggs per female) and total larval duration ranges from 2 to 3 weeks (Brazerio & Defeo, 1999). In contrast, the European intertidal species *Donacilla cornea* has been anecdotally reported as having no planktonic stage with larvae brooded in the pallial cavity, although Whiteley, Owen & Smith (1997) stated that the species has a planktonic larval stage of unknown duration.

Development to the pediveliger stage in *P. ventricosa* is comparatively slow compared with other bivalve species. In a review of bivalve development in 54 species across a temperature range of 5–26 °C, development to pediveliger in marine species was reported to take between 6 and 40 d (Ackerman *et al.*, 1994). At 20–25 °C, development of *P. ventricosa* to this stage was complete by 31 to 22 d respectively, which is slower than in commonly cultured bivalve species (e.g. 10–20 d in scallop species at the same temperatures; Cragg, 2006). While development rates depend on a range of variables besides temperature, phylogenetic differences will also be present and it is possible that slow to moderate development rates are a feature of the genus *Paphies* (i.e. 18–22 d in *P. australis*; 17 d in *P. subtriangulata*) and possibly of the Mesodematidae in general (>2–3 weeks in *Mesodesma*).

Early larval shell formation

While the morphology of embryonic and larval stages of *P. ventricosa* is typical for bivalves, there are several points of interest in shell formation in the early developmental stages, of which there is a limited understanding elsewhere. Aranda-Burgos *et al.* (2014) noted that in bivalve larva there is some uncertainty regarding the timing of shell-gland formation, and whether the process occurs at the gastrula stage or later. For *P. ventricosa*, the shell-field invagination occurs at the gastrula stage, prior to the complete formation of the prototroch (Fig. 2C). Aranda-Burgos *et al.* (2014) carefully documented the formation of the shell gland in *Ruditapes decussatus* at a similar developmental stage, as reported in *Chione cancellata* (Mouëza *et al.*, 2006) and a number of other bivalve genera (*Venus*, *Ostrea*, *Crassostrea* and *Mytilus*, see Aranda-Burgos *et al.*, 2014). In contrast, the shell field forms at the trochophore stage in *Spisula solidissima* (Eyster & Morse, 1984).

Aranda-Burgos *et al.* (2014) outlined two contrasting models of shell formation in bivalve larvae, one in which the shell-field invagination closes completely during shell production and the other in which the shell field only corresponds to the floor of the shell-field depression. Our observations are consistent with the latter process, as proposed by Mouëza *et al.* (2006) and described in *R. decussatus* by Aranda-Burgos *et al.* (2014). The expansion of the dorsal shell field in *P. ventricosa* occurs during gastrulation and early trochophore larvae have a well-developed shell field with a clearly defined axial line between the two shell lobes.

The nature of calcification in the larvae was not ascertained in the present study. In our SEM preparations of the early trochophore, the shell field had a wrinkled appearance (Fig. 2E), similar to previous observations, which has been suggested to represent noncalcified organic periostracum (Silberfeld & Gros, 2006). We also observed a wrinkled pattern in the shells of *P. ventricosa* in the straight-hinged D-larval stage; similar patterns have been seen in SEM preparations of other bivalve larvae, such as *Anomalocardia brasiliana* (Mouëza *et al.*, 2006) and *R. decussatus* (Aranda-Burgos *et al.*, 2014). These wrinkles have been attributed to shrinkage artefacts associated with dehydration during SEM preparation, and not to a lack of calcification, which is likely to be initiated at the trochophore stage (Weiss *et al.*, 2002) and can occur in the prodissoconch I shell before the formation of the organic phase is complete (LaBarbera, 1974).

Larval development and temperature

Embryonic and larval development rate in *P. ventricosa* was found to be temperature dependent within the range tested (12–20 °C), a response that is typical of bivalve larvae (Widdows, 1991; Cragg, 2006). Examples include increased rate of development with temperature in *M. edulis* (Pechenik *et al.*, 1990), *M. galloprovincialis* (Sánchez-Lazo & Martínez-Pita, 2012), *Perna viridis* (Manoj Nair & Appukuttan, 2003), *C. gigas* (Kheder, Moal & Robert, 2010), *Mytilopsis leucophaeata* (Verween, Vincx & Degraer, 2007), *Saccostrea glomerata* (Parker, Ross & O'Connor, 2009) and the freshwater species *Limnoperna fortunei* (Cataldo *et al.*, 2005). While direct comparisons among species are difficult, given the range of experimental temperatures and conditions used, the magnitude of temperature-dependence observed in *P. ventricosa* is within that observed in other bivalve larvae. For example, using the temperature quotient, Q_{10} (i.e. the change in growth rate across a 10 °C temperature difference) to compare growth responses to temperature at day 27, we observed a $Q_{10} = 1.82$ (from 12 to 16 °C) and $Q_{10} = 2.33$ (from 16 to 20 °C). These values are within the Q_{10} range reported for *M. galloprovincialis* (Sánchez-Lazo & Martínez-Pita, 2012: $Q_{10} = 0.95$ from 20 to 24 °C and $Q_{10} = 2.69$ from 17 to 20 °C), *M. edulis* (Sprung, 1984: $Q_{10} = 1.9$ from 12 to 18 °C), *Macoma balthica* (Drent, 2002: $Q_{10} = 1.5$ from 10 to 20 °C) and *Donax obesulus* (Carstensen *et al.*, 2010; $Q_{10} = 1.19$ from 17.8 to 24.6 °C). The effect of temperature on larval development is best studied in pectinids; in a review by Cragg (2006) the relationship between time to metamorphosis and temperature was quantified using an Arrhenius plot, from which the positive response to temperature (−Ea) was remarkably constant across the family.

Temperature is thought to be second only to diet in determining larval development rates (His, Robert & Dinet, 1989; Helm, Bourne & Lovatelli, 2004). Increases in development rate at higher temperatures are related to higher metabolic rates (Rico-Villa, Poureau & Robert, 2009) and potentially greater assimilation efficiency of algal diets (Manoj Nair & Appukuttan, 2003). While a positive developmental response to warmer temperatures is universal, optimal development temperatures for bivalve larvae vary among species, with ranges of 15–20 °C in *C. gigas* (Helm & Millican, 1982), 20–25 °C in *M. galloprovincialis* (His *et al.*, 1989), 17–20 °C in *M. edulis* (Hrs-Brenko & Calabrese, 1969), 22–26 °C in *S. glomerata* (Parker *et al.*, 2009) and 22 °C for *M. leucophaeata* (Verween *et al.*, 2007). We could not establish the optimal temperature for larval growth in *P. ventricosa*, but SL growth over 39 d was maximal at the highest temperature

treatment (20 °C). Redfearn (1982) observed that pediveliger larvae developed after 22 d at 25 °C, compared with 31 d at 20 °C in the present study, suggesting an optimal temperature of at least 25 °C.

Interestingly, while shell growth rates increased with increasing temperatures, the appearance of developmental stages among the three experimental temperatures suggested the opposite (Table 1), with trochophore and D-hinge larvae observed earlier at 12 and 16 °C. It is difficult to reconcile these observations, although the faster development of preveliger stages in colder temperatures is consistent with possible acclimation to the colder temperatures experienced by the southern populations at the time of spawning (i.e. 12 and 14 °C). While there are no examples of temperature acclimation in bivalve embryos and larvae across latitude (Widdows, 1991), examples do exist in other marine invertebrates (Pecorino *et al*., 2013). The observations could also suggest that the thermal response of the larvae changes with developmental stage. This has been demonstrated in larvae of *S. glomerata* (Parker *et al*., 2009). There is also evidence for changes in the thermal tolerance of developmental stages in echinoderm larvae (Hardy *et al*., 2014; Lamare *et al*., 2014) and crab zoea and megalopa stages (Storch *et al*., 2011). Indeed, changes in the response to temperature in *P. ventricosa* were noted during the development of the veliger larvae, with no apparent effect of temperature on SL increase until day 15, when there was marked divergence in larval size in the 20 °C treatment. Day 15 broadly corresponds with the transition from the straight-hinged to umbo larva, and could indicate that developmental progression is associated with changes in temperature responses.

In terms of developmental responses to temperature in *P. ventricosa*, we note that although larval size was temperature dependent, shape was little changed (Fig. 4). This suggests that the smaller size of larvae at colder temperatures simply reflects a slowing of larval development, rather than that physiological damage by low temperatures results in abnormal or altered development.

Ecological implications

The response of *P. ventricosa* larvae to temperature has implications for spatial and temporal recruitment patterns. The broad latitudinal distribution of the species means that larval develop at 12–16 and 18–25 °C in the southern and northern populations, respectively. While other factors will affect larval development in the plankton, especially phytoplankton concentration (Pechenik, 1990; Pechenik *et al*., 1990) and salinity (Widdows, 1991; Verween *et al*., 2007, Carstensen *et al*., 2010), our results suggest that spatial differences in sea temperature around New Zealand (see Grieg, Ridgway & Shakespeare, 1998) could drive important differences in the time to reach settlement, ranging from 22 d at 25 °C (Redfearn, 1982) to >39 d at 12 °C (present study). Widdows (1991) modelled the number of bivalve larvae reaching settlement as a function of development time and noted that, at a typical larval mortality rate of $M = 0.15\ d^{-1}$, there would be an order of magnitude difference in the number of larvae reaching settlement between 22 and 39 d. Recruitment of *P. ventricosa* is marked by a high degree of temporal variation (Beentjes *et al*., 2006), and, while the specific causes are unknown, sea conditions that influence the development of the larvae will clearly be important.

SUPPLEMENTARY MATERIAL

Supplementary material is available at *Journal of Molluscan Studies* online.

ACKNOWLEDGEMENTS

The authors would like to thank kaitiaki Michael Skerrett of the Murihiku Marae for granting access to the Oreti Beach population and Liz Girvan at the Otago Center for Electron Microscopy for expert assistance in SEM techniques. Additional thanks are due to staff at Environment Southland for field support and the technicians at the Portobello Marine Laboratory who helped the experiments run smoothly.

REFERENCES

ACKERMAN, J.D., BLAIR, S., NICHOLS, S.J. & CLAUDI, R. 1994. A review of the early life history of zebra mussels (*Dreissena polymorpha*): comparisons with marine bivalves. *Canadian Journal of Zoology*, **72**: 1169–1179.

ARANDA-BURGOS, J.A., COSTA, F.D., NÓVOA, S., OJEA, J. & MARTÍNEZ-PATINÓ, D. 2014. Embryonic and larval development of *Ruditapes decussatus* (Bivalvia: Veneridae): a study of the shell differentiation process. *Journal of Molluscan Studies*, **80**: 8–16.

ARELLANO, S.M. & YOUNG, C.M. 2009. Spawning, development, and the duration of larval life in a deep-sea cold-seep mussel. *Biological Bulletin*, **216**: 149–162.

BEENTJES, M.P., CARBINES, G.D. & WILLSMAN, A.P. 2006. Effects of beach erosion on abundance and distribution of toheroa (*Paphies ventricosa*) at Bluecliffs Beach, Southland, New Zealand. *New Zealand Journal of Marine and Freshwater Research*, **40**: 439–453.

BRAZERIO, A. & DEFEO, O. 1999. Effects of harvesting and density dependence on the demography of sandy beach populations: the yellow clam *Mesodesma mactroides* of Uraguay. *Marine Ecology Progress Series*, **182**: 127–135.

CARSTENSEN, D., LAUDIEN, J., SIELFELD, W., OLIVA, M.E. & ARNTZ, W.E. 2010. Early larval development of *Donax obesulus*: response to El Niño temperature and salinity conditions. *Journal of Shellfish Research*, **29**: 361–368.

CARSTENSEN, D., OLIVA, M., SIELFELD, W. & LAUDIEN, J. 2006. Larval development of *Mesodesma donacium* (Macha). Poster presented at the XXVI Congreso de Ciencias del Mar, Iquique, Chile.

CASSIE, R.M. 1955. Population studies on the toheroa, *Amphidesma ventricosum* Gray (Eulamellibranchiata). *Australian Journal of Marine and Freshwater Research*, **6**: 348–391.

CATALDO, D., BOLTOVSKOY, D., HERMOSA, J.L. & CANZI, C. 2005. Temperature-dependant rates of larval development in *Limnoperna fortunei* (Bivalvia: Mytilidae). *Journal of Molluscan Studies*, **71**: 41–46.

CHAPARRO, O.R., THOMPSON, R.J. & EMERSON, C.J. 1999. The velar ciliature in the brooded larva of the Chilean oyster *Ostrea chilensis* (Philippi, 1845). *Biological Bulletin*, **197**: 104–111.

CRAGG, S.M. 2006. Development, physiology, behaviour and ecology of scallop larvae. In: *Scallops: biology, ecology and aquaculture* (S.E. Shumway & G.J. Parsons, eds), pp. 45–122. Elsevier, Amsterdam.

DA COSTA, G., DARRIBA, S. & MARTÍNEZ-PATIÑO, D. 2008. Embryonic and larval development of *Ensis arcuatus* (Jeffreys, 1865) (Bivalvia: Pharidae). *Journal of Molluscan Studies*, **74**: 103–109.

DRENT, J. 2002. Temperature responses in larvae of *Macoma balthica* from a northerly and southerly population of the European distribution range. *Journal of Experimental Marine Biology and Ecology*, **275**: 117–129.

EYSTER, L.S. & MORSE, M.P. 1984. Early shell formation during molluscan embryogenesis, with new studies on the surf clam, *Spisula solidissima*. *American Zoologist*, **24**: 871–882.

GIBBONS, M.C. & CASTAGNA, M. 1984. Serotonin as an inducer of spawning in six bivalve species. *Aquaculture*, **40**: 189–191.

GREENWAY, J.P.C. 1972. Further data from population surveys on toheroa (Mollusca: Eulamellibranchiata) on Northland beaches, 1962–1971. *New Zealand Marine Department Fisheries Technical Report*, **85**: 33 pp.

GRIEG, M.J., RIDGWAY, N.M. & SHAKESPEARE, B.S. 1998. Sea surface temperature variations at coastal sites around New Zealand. *New Zealand Journal of Marine and Freshwater Research*, **22**: 391–400.

HARDY, N., LAMARE, M., UTHICKE, S., WOLFE, K., DOO, S.S., DWORJANYN, S. & BYRNE, M. 2014. Thermal tolerance of early development in tropical and temperate sea urchins: inferences for the tropicalisation of eastern Australia. *Marine Biology*, **161**: 395–409.

HELM, M.M., BOURNE, N. & LOVATELLI, A. 2004. *Hatchery culture of bivalves: a practical manual*. FAO Fisheries Technical Paper 471. FAO, Rome.

HELM, M.M. & MILLICAN, P.F. 1982. Experiments in the hatchery rearing of Pacific oyster, *Crassostrea gigas* (Thunberg). *Aquaculture*, **11**: 1–12.

HIRAI, S., KISHIMOTO, T., KADAM, A.L., KANATANI, H. & KOIDE, S.S. 1988. Induction of spawning and oocyte maturation by 5-hydroxytryptamine in the surf clam. *Journal of Experimental Zoology*, **245**: 318–321.

HIS, E., ROBERT, R. & DINET, A. 1989. Combined effects of temperature and salinity on fed and starved larvae of the Mediterranean mussel *Mytilus galloprovincialis* and the Japanese oyster *Crassostrea gigas*. *Marine Biology*, **100**: 455–463.

HOOKER, S. 1997. Larval and postlarval development of the New Zealand pipi, *Paphies australis* (Bivalvia: Mesodesmatidae). *Bulletin of Marine Science*, **61**: 225–240.

HRS-BRENKO, M. & CALABRESE, A. 1969. The combined effect of salinity and temperature on larvae of the mussel *Mytilus edulis*. *Marine Biology*, **4**: 224–226.

KASYANOV, V.L., KRYUCHKOVA, G.A., KULIKOVA, V.A. & MEDVEDEVA, L.A. 1998. *Larvae of marine bivalves and echinoderms*. Smithsonian Institute Libraries, Washington, DC.

KHEDER, R.B., MOAL, J. & ROBERT, R. 2010. Impact of temperature on larval development and evolution of physiological indices in *Crassostrea gigas*. *Aquaculture*, **309**: 286–289.

LABARBERA, M. 1974. Calcification of the first larval shell of *Tridacna squamosa* (Tridacnidae: Bivalvia). *Marine Biology*, **23**: 233–238.

LAMARE, M., PECORINO, D., HARDY, N., LIDDY, M., BYRNE, M. & UTHICKE, S. 2014. The thermal tolerance of crown-of-thorns (*Acanthaster planci*) embryos and bipinnaria larvae: implications for spatial and temporal variation in adult populations. *Coral Reefs*, **161**: 395–409.

LAMBERT, J.D. 2010. Development patterns in spiralian embryos. *Current Biology*, **20**: 72–77.

MANOJ NAIR, M. & APPUKUTTAN, K.K. 2003. Effect of temperature on the development, growth, survival and settlement of green mussel *Perna viridis* (Linnaeus, 1758). *Aquaculture Research*, **34**: 1037–1045.

MAUCHLY, J.M. 1940. Significance test for sphericity of a normal n-variate distribution. *Annals of Mathematical Statistics*, **11**: 204–209.

MOUËZA, M. & FRENKIEL, L. 1995. Gill ultrastructure and symbiotic bacteria in *Codakia orbicularis* (Bivalvia, Lucinidae). *Zoomorphology*, **115**: 51–61.

MOUËZA, M., GROS, O. & FRENKIEL, L. 1999. Embryonic, larval and postlarval development of the tropical clam, *Anomalocardia brasiliana* (Bivalvia, Veneridae). *Journal of Molluscan Studies*, **65**: 73–88.

MOUËZA, M., GROS, O. & FRENKIEL, L. 2006. Embryonic development and shell differentiation in *Chione cancellata* (Bivalvia, Veneridae): an ultrastructural analysis. *Invertebrate Biology*, **125**: 21–33.

PARKER, L.M., ROSS, P.M. & O'CONNOR, W.A. 2009. The effect of ocean acidification and temperature on the fertilization and embryonic development of the Sydney rock oyster *Saccostrea glomerata* (Gould 1859). *Global Change Biology*, **15**: 2123–2136.

PECHENIK, J.A. 1990. Delayed metamorphosis by larvae of benthic marine invertebrates: does it occur? Is there a price to pay? *Ophelia*, **32**: 63–94.

PECHENIK, J.A., EYSTER, L.S., WIDDOWS, J. & BAYNE, B. 1990. The influence of food concentration and temperature on growth and morphological differentiation of blue mussel *Mytilus edulis* L. larvae. *Journal of Experimental Marine Biology and Ecology*, **136**: 47–64.

PECORINO, D., LAMARE, M., BARKER, M.F. & BYRNE, M. 2013. How does embryonic and larval thermal tolerance contribute to the distribution of the sea urchin *Centrostephanus rodgersii* (Diadematidae) in New Zealand? *Journal of Experimental Marine Biology and Ecology*, **445**: 120–128.

RAPSON, A.M. 1952. The toheroa, *Amphidesma ventricosum* Gray (Eulamellibranchiata), development and growth. *Australian Journal of Marine and Freshwater Research*, **3**: 170–198.

REDFEARN, P. 1974. Biology and distribution of the toheroa, *Paphies ventricosa* (*Mesodesma*) (Gray). *Fisheries Research Bulletin*, **11**: 1–49.

REDFEARN, P. 1982. Larval shell development of the toheroa, *Paphies ventricosa* (Gray 1843) (Mactracea: Mesodesmatidae). *New Zealand Journal of Marine and Freshwater Research*, **16**: 241–252.

REDFEARN, P. 1987. Larval shell development of the northern tuatua, *Paphies subtriangulata* (Bivalvia, Mesodesmatidae). *New Zealand Journal of Marine and Freshwater Research*, **21**: 65–70.

RICO-VILLA, B., POUREAU, S. & ROBERT, R. 2009. Influence of food density and temperature on ingestion, growth and settlement of Pacific oyster larvae, *Crassostrea gigas*. *Aquaculture*, **287**: 395–401.

SÁNCHEZ-LAZO, C. & MARTÍNEZ-PITA, I. 2012. Effect of temperature on survival, growth and development of *Mytilus galloprovincialis* larvae. *Aquaculture Research*, **43**: 1127–1133.

SASTRY, A.N. 1979. Pelecypoda (excluding Ostreidae). In: *Reproduction of marine invertebrates*, *Vol. 5: Molluscs: pelecypods and lesser classes* (A.C. Geise & J.S. Pierce, eds), pp. 113–292. Academic Press, New York.

SILBERFELD, T. & GROS, O. 2006. Embryonic development of the tropical bivalve *Tivela mactroides* (Born, 1778) (Veneridae: subfamily Meretricinae): a SEM study. *Cahiers de Biologie Marine*, **47**: 243–251.

SPRUNG, M. 1984. Physiological energetics of mussel larvae (*Mytilus edulis*). I. Shell growth and biomass. *Marine Ecology Progress Series*, **17**: 283–293.

STORCH, D., FERNÁNDEZ, M., NAVARRETE, A. & PÖRTNER, H.-O. 2011. Thermal tolerance of larval stages of the Chilean kelp crab *Taliepus dentatus*. *Marine Ecology Progress Series*, **429**: 157–167.

VERWEEN, A., VINCX, M. & DEGRAER, S. 2007. The effect of temperature and salinity on the survival of *Mytilopsis leucophaeata* larvae (Mollusca, Bivalvia): the search for environmental limits. *Journal of Experimental Marine Biology and Ecology*, **348**: 111–120.

WALLER, T.R. 1981. Functional morphology and development of veliger larvae of the European oyster, *Ostrea edulis* Linné. *Smithsonian Contributions to Zoology*, **328**: 1–70.

WEISS, I.M., TUROSS, N., ADDADI, L. & WEINER, S. 2002. Mollusc larval shell formation: amorphous calcium carbonate is a precursor phase for aragonite. *Journal of Experimental Zoology*, **293**: 478–491.

WHITELEY, D.A.A., OWEN, D.F. & SMITH, D.A.S. 1997. Massive polymorphism and natural selection in *Donacilla cornea* (Poli, 1791) (Bivalvia: Mesodesmatidae). *Biological Journal of the Linnean Society*, **62**: 475–494.

WIDDOWS, J. 1991. Physiological ecology of mussel larvae. *Aquaculture*, **94**: 147–163.

ZARDUS, J.D. & MORSE, M.P. 1998. Embryogenesis, morphology and ultrastructure of the pericalymma larva of *Acila castrensis* (Bivalvia: Protobranchia: Nuculoida). *Invertebrate Biology*, **117**: 221–244.